



HAL
open science

Free bosons with a localized source

P. L. Krapivsky, Kirone Mallick, Dries Sels

► **To cite this version:**

P. L. Krapivsky, Kirone Mallick, Dries Sels. Free bosons with a localized source. *J.Stat.Mech.*, 2020, 2006, pp.063101. 10.1088/1742-5468/ab8118 . hal-02894384

HAL Id: hal-02894384

<https://hal.science/hal-02894384>

Submitted on 21 Apr 2023

HAL is a multi-disciplinary open access archive for the deposit and dissemination of scientific research documents, whether they are published or not. The documents may come from teaching and research institutions in France or abroad, or from public or private research centers.

L'archive ouverte pluridisciplinaire **HAL**, est destinée au dépôt et à la diffusion de documents scientifiques de niveau recherche, publiés ou non, émanant des établissements d'enseignement et de recherche français ou étrangers, des laboratoires publics ou privés.

Free bosons with a localized source

P L Krapivsky^{1,2}, Kirone Mallick³ and Dries Sels^{4,5,6}

¹ Department of Physics, Boston University, Boston, Massachusetts 02215
United States of America

² Theoretical Division and CNLS, Los Alamos National Laboratory, Los
Alamos, New Mexico 87545, United States of America

³ Institut de Physique Théorique, Université Paris-Saclay, CEA and CNRS,
91191 Gif-sur-Yvette, France

⁴ Theory of quantum and complex systems, Universiteit Antwerpen, B-2610
Antwerpen, Belgium

⁵ Department of Physics, Harvard University, Cambridge, Massachusetts
02138, United States of America

E-mail: pkrapivsky@gmail.com, kirone.mallick@ipht.fr and
dsels@g.harvard.edu

Received 19 November 2019

Accepted for publication 5 March 2020

Published 9 June 2020



Online at stacks.iop.org/JSTAT/2020/063101

<https://doi.org/10.1088/1742-5468/ab8118>

Abstract. We analyze the time evolution of an open quantum system driven by a localized source of bosons. We consider non-interacting identical bosons that are injected into a single lattice site and perform a continuous time quantum walks on a lattice. We show that the average number of bosons grows exponentially with time when the input rate exceeds a certain lattice-dependent critical value. Below the threshold, the growth is quadratic in time, which is still much faster than the naive linear in time growth. We compute the critical input rate for hyper-cubic lattices and find that it is positive in all dimensions d except for $d = 2$ where the critical input rate vanishes—the growth is always exponential in two dimensions. To understand the exponential growth, we construct an explicit microscopic Hamiltonian model which gives rise to the open system dynamics once the bath is traced out. Exponential growth is identified with a region of dynamic instability of the Hamiltonian system.

Keywords: quantum dissipative systems, solvable lattice models

(Some figures may appear in colour only in the online journal)

⁶Author to whom any correspondence should be addressed.

Contents

1. Introduction	2
2. One dimension: total number of bosons	5
2.1. The supercritical regime: $\Gamma > 2$	8
2.2. The critical case: $\Gamma = 2$	8
2.3. The subcritical regime: $0 < \Gamma < 2$	10
3. Density profile in one dimension	10
3.1. The supercritical case: $\Gamma > 2$	11
3.2. The subcritical domain: $0 < \Gamma < 2$	12
3.3. The critical regime: $\Gamma = 2$	14
4.1. Two dimensions	16
4.2. High dimensions	17
4.2.1. The supercritical regime: $\Gamma > \Gamma_d$	18
4.2.2. The critical case: $\Gamma = \Gamma_d$	19
4.2.3. The subcritical domain: $\Gamma < \Gamma_d$	20
5. Density profile in high dimensions	20
6. Microscopic model	23
7. Conclusions	25
Acknowledgments	26
References	26

1. Introduction

We investigate the behavior of an open quantum system of non-interacting identical bosons driven by a localized source of bosons. We start with an empty system and assume that at time $t = 0$ the source is turned on and identical bosons are injected at a constant rate at the origin.

The evolution of open quantum systems is described by the Lindblad equation [1–4]

$$\partial_t \rho = -i [H, \rho] + 2L\rho L^\dagger - \{L^\dagger L, \rho\} \quad (1)$$

for the density matrix $\rho(t)$. The curly brackets in equation (1) denote the anti-commutator, $i = \sqrt{-1}$ and we set $k = 1$. The last two terms on the right-hand side of (1) represent a shorthand writing of a sum $\sum_{\alpha} 2L_{\alpha}\rho L_{\alpha}^{\dagger} - \{L_{\alpha}^{\dagger}L_{\alpha}, \rho\}$, with operators

L_α describing e.g. interactions with reservoirs; more generally, α labels various dissipative channels. The Lindblad equation defines the general Markovian time evolution, and it has found applications in numerous areas of quantum physics, e.g. in quantum optics [5, 6] and quantum information theory [7, 8]. Extensions of the Lindblad equation description involving more general Markovian quantum stochastic dynamics (see e.g. [9, 10]) as well as non-Markovian dynamics (see [11] for a review) have also been investigated.

Open quantum systems with time-independent Lindblad operators have been often studied. In such conditions, a unique stationary limiting state $\rho^{ss} = \rho(\infty)$ is reached and the relaxation to this state is well understood [12]. For periodic driving the system usually approaches a unique limit cycle, see e.g. [13, 14]. We consider a quench-type setup in which Lindblad operators suddenly change at a certain moment. The stationary state is never reached in our system, e.g. the total number of particles diverge as $t \rightarrow \infty$. To avoid unnecessary complications we analyze the situation when bosons are injected into a single site. Thus we have a single Lindblad operator

$$L = \begin{cases} 0 & t < 0 \\ \sqrt{\Gamma} b_0^\dagger & t > 0 \end{cases} \quad (2)$$

modeling the input at the origin with intensity Γ that is turned on at time $t = 0$. Equations (1) and (2) provide a mathematical framework for a sudden quench protocol, but instead of the change of a Hamiltonian or temperature which is usually investigated the Lindblad operator is changed in our model. For fermions, this sudden quenched protocol has been studied in [15] in the lattice realization and in [16, 17] in the continuous setting. For bosons, the problem of localized losses has been investigated both theoretically [18–23] and experimentally [24, 25], and it is dual to the problem we consider here as instead of a sink we consider a source. For fermions there is essentially no difference between a source and a sink because a particle sink is the same as a source of holes. However, for bosons a particle source and sink behave in a dramatically different way. While a phase transition can be observed in the case of losses [23, 24], such a transition is driven by a competition between interaction and dissipation. Here we show there is a rather dramatic phase transition even for free bosons if one considers an incoherent source, rather than a sink.

We consider free lattice bosons, so the Hamiltonian appearing in equation (1) admits a simple expression, $H = \sum_{\langle i,j \rangle} b_i^\dagger b_j + b_j^\dagger b_i$, through creation and annihilation operators, where the sum is taken over pairs of neighboring lattice sites i and j . The non-trivial commutators are $b_i, b_j^\dagger = \delta_{i,j}$, all other commutators vanish. We focus on uniform systems, so the hopping rates are equal and we set them to unity.

A basic characteristic of this open quantum system is the total number $N(t)$ of bosons at time t . The full statistics of this evolving random quantity is described by the probability distribution $P(N, t) = \text{Prob}[N(t) = N]$. The exploration of the full statistics is a challenging problem which is left for the future; here we focus on the

average total number of bosons $N(t)$ and on the density of bosons. These characteristics are encoded in the two-point correlation function

$$\sigma_{i,j}(t) = \langle b_i^\dagger b_j \rangle = \text{Tr} \rho(t) b_i^\dagger b_j \quad (3)$$

We limit ourselves to hyper-cubic lattices \mathbb{Z}^d , so we have just two dimensionless parameters, Γ and d . We focus on the long time behavior, $t \gg 1$. One anticipates a linear growth of $N(t)$, more precisely

$$N_{\text{naive}}(t) = 2\Gamma t \quad (4)$$

This naive growth law would be exact in arbitrary dimension if non-interacting particles were distinguishable. Quantum statistics induces effective repulsion of identical fermions and attraction of identical bosons, so one expects (4) to provide an upper bound for fermions and a lower bound for bosons. This is indeed correct. Furthermore, we have recently shown [15] that the asymptotic growth is linear in time for fermions. More precisely, $N(t) = c_d(\Gamma)t$ with $c_d(\Gamma) < 2\Gamma$ and $\Gamma^{-1}c_d(\Gamma) \rightarrow 2$ as $\Gamma \rightarrow +0$. For bosons, in contrast, the lower bound (4) is essentially useless as the actual asymptotic growth of $N(t)$ is super-linear. Below we show that this growth is remarkably rich: a dynamical phase transition between algebraic and exponential growth occurs when the input rate passes through the critical value. In one dimension, the critical input rate is $\Gamma_1 = 2$ and

$$N(t) \simeq \begin{cases} A_1(\Gamma) e^{2t \sqrt{\Gamma^2 - 4}} & \Gamma > 2 \\ \frac{64}{3} t^4 & \Gamma = 2 \\ B_1(\Gamma) t^2 & \Gamma < 2 \end{cases} \quad (5)$$

with amplitudes

$$A_1(\Gamma) = \frac{\Gamma^4}{(\Gamma^2 - 4)^2} \quad (6a)$$

$$B_1(\Gamma) = \frac{4\Gamma^4}{4 - \Gamma^2} \quad (6b)$$

When $d \geq 3$, the asymptotic behaviors of the average total number of bosons are rather similar to that for the one-dimensional case:

$$N(t) \simeq \begin{cases} A_d(\Gamma) e^{2C_d(\Gamma)t} & \Gamma > \Gamma_d \\ B_d^{\text{crit}} t^2 & \Gamma = \Gamma_d \\ B_d(\Gamma) t^2 & \Gamma < \Gamma_d \end{cases} \quad (7)$$

The only difference with the one-dimensional growth laws represented by equation (5) is that the time dependence in the critical regime is the same as in the sub-critical regime, $N \propto t^2$; the amplitude undergoes a phase transition, $B_d^{\text{crit}} = B_d(\Gamma_d)$.

The two-dimensional case is exceptional: the critical input rate vanishes, $\Gamma_2 = 0$, and hence the exponential growth, $A_2(\Gamma) e^{2C_2(\Gamma)t}$, occurs for all $\Gamma > 0$. The critical input rate seems to vanish for all two-dimensional lattices, reflecting the peculiar role of $d = 2$.

In section 2 we analyze the behavior in one dimension and establish the growth law (5). The density profile in one dimension is derived in section 3. Section 4 analyzes the behavior in higher dimensions. The density profile in higher dimensions is investigated in section 5. An explicit microscopic Hamiltonian model for the system, including a bath, is constructed in section 6. Conclusions are given in section 7.

2. One dimension: total number of bosons

In one dimension, the Hamiltonian reads

$$H = \sum_{n=-\infty}^{\infty} b_n^\dagger b_{n+1} + b_{n+1}^\dagger b_n \quad (8)$$

An exact solution for the density matrix ρ is an intriguing challenge which is left to future work. Here we focus on the two-point correlation function

$$\sigma_{i,j}(t) = \text{Tr} \rho(t) b_i^\dagger b_j \quad (9)$$

Using the Lindblad equation (1) with Hamiltonian (8) and $L = \sqrt{\Gamma} b_0^\dagger$ we deduce a closed system of coupled differential equations

$$\frac{d\sigma_{i,j}}{dt} = i(\sigma_{i+1,j} + \sigma_{i-1,j} - \sigma_{i,j+1} - \sigma_{i,j-1}) + \Gamma(\delta_{i,0}\sigma_{i,j} + \delta_{j,0}\sigma_{i,j}) + 2\Gamma\delta_{i,0}\delta_{j,0} \quad (10)$$

for the two-point correlation function. This infinite system of linear equations admits an exact solution. To derive this solution we first drop the source term, viz. the term in the second line in (10), solve the resulting *homogeneous* system of equations, and then express the solution of (10) through the solution of the homogeneous system. Thus we start with

$$\frac{d\sigma_{i,j}}{dt} = i(\sigma_{i+1,j} + \sigma_{i-1,j} - \sigma_{i,j+1} - \sigma_{i,j-1}) + \Gamma(\delta_{i,0}\sigma_{i,j} + \delta_{j,0}\sigma_{i,j}) \quad (11)$$

The factorization ansatz

$$\sigma_{i,j}(t) = S_i(t)S_j^*(t) \quad (12)$$

is consistent with (11) if the functions $S_n(t)$ satisfy

$$\frac{dS_n}{dt} = i[S_{n+1} + S_{n-1}] + \Gamma\delta_{n,0}S_n \quad (13)$$

Similar equations have been analyzed in [15, 26]; below we employ the same procedure.

A proper choice of the initial condition which will allow us to treat the original system (10) starting from the empty lattice is

$$S_n(0) = \delta_{n,0} \quad (14)$$

The solution of the initial-value problem (13) and (14) can be obtained using the Laplace–Fourier transform. The Laplace transform with respect to time,

$$\hat{S}_n(s) = \int_0^\infty e^{-st} S_n(t) dt, \tag{15}$$

recasts (13) into

$$s\hat{S}_n - \delta_{n,0} = i\hat{S}_{n+1} + i\hat{S}_{n-1} + \Gamma\delta_{n,0}\hat{S}_n \tag{16}$$

Performing the Fourier transform in space,

$$S(s, q) = \sum_{n=-\infty}^{\infty} \hat{S}_n(s) e^{-iqn}, \tag{17}$$

we obtain

$$S(s, q) = \frac{1 + \Gamma\hat{S}_0(s)}{s - 2i \cos q} \tag{18}$$

The definition (17) implies

$$\hat{S}_0(s) = \frac{1}{2\pi} \int_0^{2\pi} dq S(s, q)$$

which in conjunction with (18) fixes

$$\hat{S}_0(s) = \sqrt{\frac{1}{s^2 + 4 - \Gamma}} \tag{19}$$

and yields

$$S(s, q) = \frac{\sqrt{s^2 + 4}}{s^2 + 4 - \Gamma} \frac{1}{s - 2i \cos q} \tag{20}$$

Inverting the Fourier transform we arrive at

$$\hat{S}_n(s) = \sqrt{\frac{1}{s^2 + 4 - \Gamma}} \frac{\sqrt{2i}}{s + \sqrt{s^2 + 4}} |n| \tag{21}$$

Returning to the original problem we note that equation (10) can be rewritten as

$$\dot{\sigma} = M\sigma + V \tag{22}$$

where $\sigma = \sigma(t)$ is an infinite vector with components $\sigma_{i,j}(t)$, the matrix M encodes the homogeneous terms, and the source term V is a vector with a unique non-zero component, $2\Gamma\delta_{i,0}\delta_{j,0}$. Solving (22) gives

J. Stat. Mech. (2020) 063101

$$\sigma(t) = \int_0^t d\tau e^{(t-\tau)M} V \quad (23)$$

Noting that e^{tM} is the solution of the initial-value problem (13) and (14) and using the ansatz (12) we establish

$$\sigma_{i,j}(t) = 2\Gamma \int_0^t d\tau S_i(\tau) S_j^*(\tau) \quad (24)$$

with functions S_i satisfying the dynamics (13).

The average total number of particles is

$$N(t) = \sum_{n=-\infty}^{\infty} \sigma_{n,n}(t) \quad (25)$$

Combining this result with (24) we obtain

$$N(t) = 2\Gamma \int_0^t d\tau \sum_{n=-\infty}^{\infty} |S_n(\tau)|^2 \quad (26)$$

Using (13) we express the sum in (26) through $S_0(t)$:

$$\sum_{n=-\infty}^{\infty} |S_n(t)|^2 = 1 + 2\Gamma \int_0^t dt' |S_0(t')|^2 \quad (27)$$

Differentiating (26) and using (27) we arrive at

$$\frac{dN}{dt} = 2\Gamma \left(1 + 2\Gamma \int_0^t dt' |S_0(t')|^2 \right) \quad (28)$$

from which $N(t) \geq 2\Gamma t$. Thus (4) indeed provides the lower bound as we have asserted. Differentiating (28) we obtain

$$\frac{d^2N}{dt^2} = (2\Gamma)^2 |S_0(t)|^2 \quad (29)$$

which we shall also use below.

The Laplace transform (19) has a neat form, but inverting it in terms of special functions appears impossible. A rather simple integral representation of $S_0(t)$ is possible, however. To derive it we rely on a useful general identity for inverse Laplace transforms. Suppose we know the inverse Laplace transform $f(t)$ of $\hat{f}(s)$, but we actually want to determine the inverse Laplace transform $F(t)$ of $\hat{F}(s) \equiv \frac{\hat{f}(s)}{s^2 + a^2}$. This inverse Laplace transform admits [27] a general expression through $f(t)$,

$$F(t) = f(t) - a \int_0^t d\tau J_1(a\tau) f \frac{\sqrt{t^2 - \tau^2}}{t^2 - \tau^2}, \quad (30)$$

where J_1 is the Bessel function. Specializing to (19) we obtain

$$S_0(t) = e^{\Gamma t} - 2 \int_0^t d\tau J_1(2\tau) e^{\Gamma \sqrt{t^2 - \tau^2}} \quad (31)$$

The integral representation (31) is useful for extracting the small time behavior:

$$\mathcal{S}(t) = 1 + \Gamma t + \frac{1}{2} \Gamma^2 t^2 - \frac{1}{6} \Gamma^3 t^3 + \frac{1}{24} \Gamma^4 t^4 - 6\Gamma^2 t^4 + \dots$$

Combining this expansion with (28) we obtain

$$N = 2\Gamma t + 2\Gamma^2 t^2 + \frac{4}{3} \Gamma^3 t^3 + \frac{2}{3} \Gamma^2 (\Gamma^2 - 1) t^4 + \frac{2}{15} \Gamma^2 (2\Gamma^2 - 5) t^5 + \frac{1}{45} \Gamma^2 (4\Gamma^4 - 17\Gamma^2 + 9) t^6 + \dots \quad (32)$$

The leading small time asymptotic is linear in time in agreement with intuition. The lower bound (4) actually provides the leading small time asymptotic.

The large time growth is faster than linear as we show below. The leading behavior in the $t \rightarrow \infty$ limit is easier to extract directly from the Laplace transform (19) than from the integral representation (31).

2.1. The supercritical regime: $\Gamma > 2$

To determine the leading large time behavior of $S_0(t)$ when the source is sufficiently strong, $\Gamma > 2$, it is useful to re-write (19) as

$$\hat{S}_0(s) = \frac{1}{s - \sqrt{\Gamma^2 - 4s}} \frac{\sqrt{s^2 + 4 + \Gamma}}{\sqrt{\Gamma^2 - 4}} \quad (33)$$

This Laplace transform has a simple pole at $s = \frac{\sqrt{\Gamma^2 - 4}}{2}$ with residue $\frac{\Gamma}{\sqrt{\Gamma^2 - 4}}$. Therefore the asymptotic growth of $S_0(t)$ is exponential

$$S_0(t) \simeq \frac{\Gamma}{\sqrt{\Gamma^2 - 4}} e^{t \frac{\sqrt{\Gamma^2 - 4}}{2}} \quad (34)$$

and the total number of bosons found from (29) and (34) is also exponential

$$N(t) \simeq \frac{\Gamma^4}{(\Gamma^2 - 4)^2} e^{2t \frac{\sqrt{\Gamma^2 - 4}}{2}} \quad (35)$$

This is the announced asymptotic, (5) and (6a), in the $\Gamma > 2$ region.

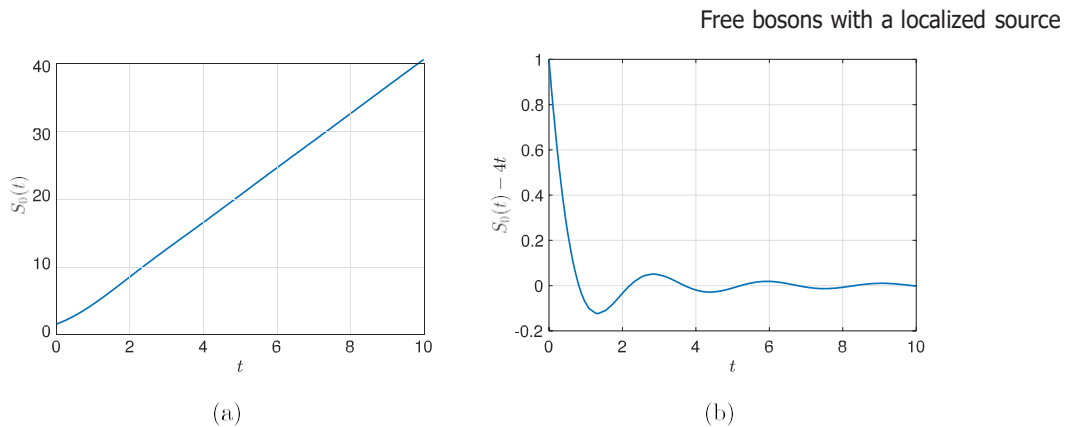


Figure 1. (a) $S_0(t)$ versus time t ; we compute S_0 using the integral representation (31) with $\Gamma = 2$. (b) The deviation $S_0(t) - 4t$ from the leading asymptotic approaches to zero in an oscillatory manner.

2.2. The critical case: $\Gamma = 2$

The Laplace transform (33) simplifies to

$$\hat{S}_0(s) = \frac{\sqrt{s^2 + 4} + 2}{s^2} \tag{36}$$

and behaves as $4/s^2$ when $s \rightarrow 0$, implying that $S_0(t) \simeq 4t$ as $t \rightarrow \infty$, see also figure 1(a). Plugging $S_0(t) \simeq 4t$ into (29) we obtain the announced asymptotic (5) at $\Gamma = 2$, namely

$$N(t) \simeq \frac{64}{3} t^4 \tag{37}$$

Figure 1(b) shows that $S_0(t) - 4t$ approaches to zero in an oscillatory manner. To derive this sub-leading correction analytically, we re-write (36) as

$$\hat{S}_0(s) = \frac{4}{s^2} + \hat{F}_*(s), \quad \hat{F}_*(s) = \sqrt{\frac{1}{s^2 + 4} + 2} \tag{38}$$

Performing the inverse Laplace transform and using the identity (30) we establish an integral representation

$$S_0(t) - 4t = F_*(t), \quad F_*(t) = e^{-2t} - 2 \int_0^t d\tau J_1(2\tau) e^{-2\tau} \frac{\sqrt{2-\tau}}{t-\tau} \tag{39}$$

The leading long-time behavior is now readily computed:

$$S_0(t) - 4t \simeq - \frac{J_1(2t)}{2t} \simeq \frac{\cos \sqrt{2t + \frac{\pi}{4}}}{\sqrt{4\pi t^3}} \tag{40}$$

for $t \gg 1$. Using (28) we find that the sub-leading correction to the asymptotic growth law (37) scales linearly with time:

$$N(t) - \frac{64}{3} t^4 \simeq 4(1 + f_*)t, \quad f_* = 4 \int_0^\infty dt F_*(t) [F_*(t) + 8t] \tag{41}$$

2.3. The subcritical regime: $0 < \Gamma < 2$

To determine the asymptotic behavior of $S_0(t)$ when the source is sufficiently weak, $\Gamma < 2$, it is useful to re-write (19) as

$$\hat{S}_0(s) = \frac{\sqrt{s^2 + 4 + \Gamma}}{s^2 + 4 - \Gamma^2} \quad (42)$$

This Laplace transform has poles at $s = \pm i\sqrt{4 - \Gamma^2}$. The contribution of these poles to the inverse Laplace transform

$$S_0(t) \simeq \sqrt{\frac{2\Gamma}{4 - \Gamma^2}} \sin t \sqrt{4 - \Gamma^2} \quad (43)$$

is asymptotically dominant. Therefore

$$\int_0^t dt' |S_0(t')|^2 \simeq \frac{2\Gamma^2}{4 - \Gamma^2} t \quad (44)$$

which in conjunction with (28) leads to the announced asymptotic, (5) and (6b), in the $\Gamma < 2$ region.

The sub-leading correction is determined using the same procedure as in the critical case, cf (38) and (39). Namely we write

$$\hat{S}_0(s) = \frac{2\Gamma}{s^2 + 4 - \Gamma^2} + \hat{F}(s), \quad \hat{F}(s) = \frac{\sqrt{s^2 + 4 - \Gamma}}{s^2 + 4 - \Gamma^2} \quad (45)$$

from which we deduce an integral representation of the sub-leading correction

$$F(t) = e^{-\Gamma t} - 2 \int_0^t d\tau J_1(2\tau) e^{-\Gamma \sqrt{t - \tau}} \quad (46)$$

which leads to

$$S_0(t) - \sqrt{\frac{2\Gamma}{4 - \Gamma^2}} \sin t \sqrt{4 - \Gamma^2} \simeq \frac{2}{\Gamma^2} \frac{\cos \sqrt{2t + \frac{\pi}{4}}}{\pi t^3} \quad (47)$$

Straight forward calculations lead to the following more accurate asymptotic expansion for the average number of bosons,

$$N(t) = B_1(\Gamma)t^2 + 2\Gamma[1 + f(\Gamma)]t + \frac{4\Gamma^4}{(4 - \Gamma^2)^2} \cos \sqrt{2t + \frac{\pi}{4}} \quad (48)$$

with

$$f(\Gamma) = 2\Gamma \int_0^\infty dt F^2(t) + \sqrt{\frac{8\Gamma^2}{4 - \Gamma^2}} \int_0^\infty dt F(t) \sin t \sqrt{4 - \Gamma^2} \quad (49)$$

where $F(t)$ is given by (46).

3. Density profile in one dimension

Let us first determine the density at the origin $\rho_0(t) \equiv \sigma_{0,0}(t)$. Equation (24) shows that

$$\rho_0(t) = 2\Gamma \int_0^t dt' |S_0(t')|^2 \quad (50)$$

Using already established results for $S_0(t)$ we arrive at the asymptotic behaviors

$$\rho_0(t) \simeq \begin{cases} a_1(\Gamma) e^{2t \sqrt{\Gamma^2 - 4}} & \Gamma > 2 \\ \frac{64}{3} t^3 & \Gamma = 2 \\ b_1(\Gamma) t & \Gamma < 2 \end{cases} \quad (51)$$

with amplitudes

$$a_1(\Gamma) = \sqrt{\frac{\Gamma}{\Gamma - 4}}^3 \quad (52a)$$

$$b_1(\Gamma) = \frac{4\Gamma^3}{4 - \Gamma^2} \quad (52b)$$

A more accurate long time behavior of the density at the origin can be established using results of the previous section. When $\Gamma = 2$

$$\rho_0(t) = \frac{64}{3} t^3 + f_* + O(t^{-1/2}) \quad (53)$$

with f_* appearing in (41), while for $\Gamma < 2$

$$\rho_0(t) = b_1(\Gamma) t - 2 \sqrt{\frac{\Gamma}{4 - \Gamma^2}}^3 \sin 2t \sqrt{\frac{\Gamma}{4 - \Gamma^2}} + f(\Gamma) + O(t^{-3/2}) \quad (54)$$

with $f(\Gamma)$ given by (49).

We now analyze the entire density profile.

3.1. The supercritical case: $\Gamma > 2$

To determine the asymptotic behavior of $S_n(t)$ in the super-critical regime, $\Gamma > 2$, we guess that $S_n(t)$ exhibits the same exponential growth as $S_0(t)$, see (34), that is

$$S_n(t) \simeq F_n e^{t \sqrt{\Gamma^2 - 4}} \quad (55)$$

Plugging this ansatz into (13) we obtain

$$\sqrt{\Gamma^2 - 4} F_n = i [F_{n+1} + F_{n-1}] \quad (56)$$

for $n \neq 0$. Solving this simple recurrence yields⁷

$$F_n = C i^{|n|} \frac{\Gamma \sqrt{\Gamma^2 - 4}^{|n|}}{2^{|n|}} \quad (57)$$

At the origin the recurrence (56) should be modified to

$$\sqrt{\Gamma^2 - 4} F_0 = i [F_1 + F_{-1}] + \Gamma F_0 \quad (58)$$

One can verify that (58) is consistent with the exact solution (57).

Recalling (24) we have

$$\rho_n(t) \equiv \sigma_{n,n}(t) = 2\Gamma \int_0^t d\tau S_n(\tau) S_n^*(\tau) \quad (59)$$

Combining this result with (55) and (57) we compute the density. Matching with already known density at the origin we obtain

$$\frac{\rho_n(t)}{\rho_0(t)} = \frac{\Gamma \sqrt{\Gamma^2 - 4}^{|2n|}}{2^{|2n|}} \quad (60)$$

Thus the density profile normalized to its value at the origin is purely exponential in the super-critical regime. Re-writing (60) as

$$\rho_n(t) = a_1(\Gamma) \exp \left(2 \ln \frac{\Gamma + \sqrt{\Gamma^2 - 4}}{2} [Vt - |n|] \right) \quad (61)$$

with

$$V = \frac{\sqrt{\Gamma^2 - 4}}{\Gamma + \sqrt{\Gamma^2 - 4}} \ln \frac{\Gamma + \sqrt{\Gamma^2 - 4}}{2} \quad (62)$$

we conclude that the interval $[-Vt, Vt]$ is filled with bosons, and at most few bosons are outside of this interval. The speed V of the extension of the droplet of bosons exceeds the genuine speed, 2 in our units, with which a single continuous time quantum walker would have spread (see figure 2). This excess is caused by the exponential growth of the total number of bosons—the exponentially small spills over the natural $\pm 2t$ boundaries for each quantum walker accumulate to increase the speed to $V(\Gamma) > 2$.

The extremal behaviors of the speed are

$$V = 2 + \frac{1}{\Gamma^3} (\Gamma - 2) - \frac{1}{90} \frac{1}{(\Gamma - 2)^2} + \dots (\Gamma \rightarrow 2 + 0) \quad (63a)$$

$$V = \frac{1}{\ln \Gamma} - \frac{1}{\Gamma \ln \Gamma} + \frac{1}{\Gamma (\ln \Gamma)^2} + \dots (\Gamma \rightarrow \infty) \quad (63b)$$

⁷We keep only the solution that vanishes when $|n| \rightarrow \infty$.

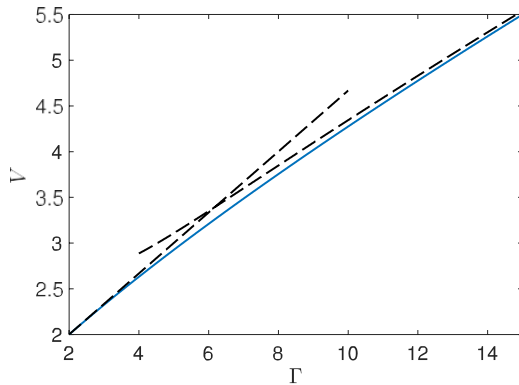


Figure 2. The speed V of the extension of the droplet of bosons versus the input rate Γ in one dimension in the supercritical regime. The analytical prediction for the speed is given by (62); dashed lines show asymptotic results.

3.2. The subcritical domain: $0 < \Gamma < 2$

In the sub-critical regime, $0 < \Gamma < 2$, we have $\rho_n \sim \rho_0 \sim t$ which is consistent with (59) when $S_n = O(1)$. More precisely, $S_n(t)$ is expected to admit a scaling form

$$S_n(t) \simeq i^{|n|} S(v), \quad v = \frac{n}{2t} \tag{64}$$

in the scaling limit

$$|n| \rightarrow \infty, t \rightarrow \infty, \quad v = \frac{n}{2t} = \text{finite} \tag{65}$$

Inserting (64) into (13) and replacing the difference $S[v - 1/(2t)] - S[v + 1/(2t)]$ by derivative $t^{-1} \frac{dS}{dv}$ we arrive at a simple equation $(1 - v) \frac{dS}{dv} = 0$ for the scaling function $S(v)$. Therefore $S(v)$ is a constant, more precisely

$$S = C \times \begin{cases} 1 & |v| < v_* \\ 0 & |v| > v_* \end{cases} \tag{66}$$

We expect $v_* \leq 1$ since bosons propagate at most on distance $\pm 2t$ from the origin. Plugging (66) into (59) we obtain

$$\begin{aligned} \rho_n &= \begin{cases} 1 - |v|/v_* & |v| < v_* \\ 0 & |v| > v_* \end{cases} \\ \rho_0 &= 0 \end{aligned} \tag{67}$$

Using this profile we compute the total number of bosons $N = \rho_0 v_* 2t$. Combining this with known asymptotic behaviors

$$N = \frac{4\Gamma^4}{4 - \Gamma^2} t^2, \quad \rho_0 = \frac{4\Gamma^3}{4 - \Gamma^2} t$$

J. Stat. Mech. (2020) 063101

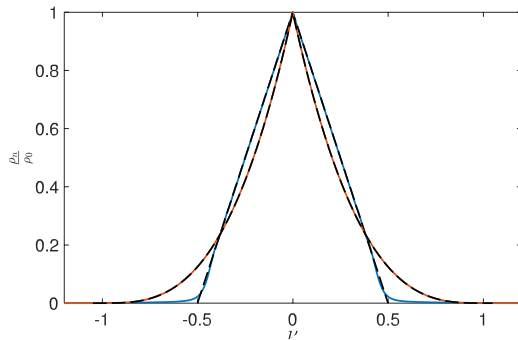


Figure 3. The density profile normalized to its value at the origin in the sub-critical regime (the profile at $\Gamma = 1$ is shown in blue) and in the critical regime ($\Gamma = 2$) in red. The dashed lines show the analytic asymptotic results and the full lines are numeric results computed at $t = 400$.

J. Stat. Mech. (2020) 063101

we fix $\nu_* = \Gamma/2$. Thus in the subcritical regime the asymptotic density profile normalized to its value at the origin is

$$\frac{\rho_n}{\rho_0} = \begin{cases} 1 - 2|\nu|/\Gamma & |\nu| < \Gamma/2 \\ 0 & |\nu| > \Gamma/2 \end{cases} \quad (68)$$

This tent-like density profile is shown in figure 3.

3.3. The critical regime: $\Gamma = 2$.

In the critical regime, $\rho_n \sim \rho_0 \sim t^3$ which is consistent with (59) when $S_n = O(t)$. More precisely, the density admits the scaling form

$$S_n(t) \simeq i^n t S(\nu), \quad \nu = \frac{n}{2t} \quad (69)$$

in the scaling limit (65). Plugging (69) into (13) we arrive at the differential equation $(1 - \nu)S' = -S$ which is solved to give⁸

$$S = C \times \begin{cases} 1 - |\nu| & |\nu| < 1 \\ 0 & |\nu| > 1 \end{cases} \quad (70)$$

Using (69) and (70) we compute the integral in (59)

$$\rho_n = 4C^2 \int_{n/2}^t dt \tau^2 (1 - \nu)^2 = \frac{4C^2}{3} t - \frac{n}{2}^3$$

Thus the asymptotic density profile normalized to its value at the origin is

⁸Our analysis is performed in the region $0 < \nu \leq 1$. The solution for $-1 \leq \nu < 0$ is determined by symmetry. There are essentially no bosons in the $|\nu| > 1$ region.

$$\frac{\rho_n(t)}{\rho_0(t)} = (1 - |v|)^3, \quad \rho_0(t) = \frac{64}{3} t^3 \quad (71)$$

in the critical regime. This cubic density profile is shown in figure 3.

4. Free bosons on Z^d with a source

Here we consider non-interacting identical bosons performing independent continuous time quantum walks on Z^d and coupled to a source at the origin. As in one dimension, we first drop the source term in equations for $\sigma_{i,j}(t)$ and use the factorization ansatz. We then perform the Laplace transform for quantities $S_n(t)$

$$\hat{S}_n(s) = \int_0^\infty S_n(t) e^{-st} dt \quad (72a)$$

followed by the Fourier transform

$$S(s, \mathbf{q}) = \sum_n \hat{S}_n(s) e^{-i\mathbf{q} \cdot \mathbf{n}} \quad (72b)$$

Here $\mathbf{n} = (n_1, \dots, n_d)$, $\mathbf{q} = (q_1, \dots, q_d)$ and $\mathbf{q} \cdot \mathbf{n} = q_1 n_1 + \dots + q_d n_d$. We shortly write

$$\sum_n = \sum_{n_1=-\infty}^{\infty} \dots \sum_{n_d=-\infty}^{\infty} \quad (73a)$$

$$\int d\mathbf{q} = \int_0^{2\pi} \frac{dq_1}{2\pi} \dots \int_0^{2\pi} \frac{dq_d}{2\pi} \quad (73b)$$

We also define

$$\Psi_d(s, \mathbf{q}) = \prod_{\alpha=1}^d \sum_{q_\alpha} \#_{-1} \cos q_\alpha \quad (74a)$$

$$\Phi_d(s) = \int d\mathbf{q} \Psi_d(s, \mathbf{q})^{-1} \quad (74b)$$

Equation (74b) expresses $\Phi_d(s)$ through a d -fold integral. This multiple integral can be reduced to a single integral involving a Bessel function:

$$\Phi_d(s) = \int_0^\infty du e^{-us} [J_0(2u)]^d \quad (75)$$

This is established using (74a) and (74b) and the well-known integral representation

$$J_0(z) = \int_0^{2\pi} \frac{dq}{2\pi} e^{2zi \cos q} \quad (76)$$

of the Bessel function.

Applying the Laplace–Fourier transform to the governing equations we arrive at

$$S(s, q) = \frac{1}{1 + \Gamma \hat{S}_0(s)} \Psi_d(s, q) \quad (77)$$

From the definition (72b), we obtain

$$\hat{S}_0(s) = \int dq S(s, q) \quad (78)$$

Using (77) and (78) we find that

$$\hat{S}_0(s) = [\Phi_d(s) - \Gamma]^{-1} \quad (79)$$

with $\Phi_d(s)$ defined in (74b). Therefore (77) becomes

$$S(s, q) = \frac{\Phi_d(s)}{\Phi_d(s) - \Gamma} \Psi_d(s, q) \quad (80)$$

Similarly to one dimension, the growth of the total average number of bosons is governed by the differential equation

$$\frac{d^2 N}{dt^2} = (2\Gamma)^2 |S_0(t)|^2 \quad (81)$$

4.1. Two dimensions

For the square lattice, the integral in equation (75) admits a representation through a simpler integral (see [28])

$$\Phi_2(s) = \frac{\pi}{2} \int_0^{\pi/2} \frac{d\vartheta}{\sqrt{s^2 + 16\sin^2\vartheta}} \quad (82)$$

The integral in (82) can be expressed through complete elliptic integrals, but the form (82) suffices for us. As in one dimension where $\Phi_1(s) = \sqrt{s^2 + 4}$, the function $\Phi_2(s)$ is a monotonically increasing function of s . The key difference from the one-dimensional case is that $\Phi_2(0) = 0$ and hence $\hat{S}_0(s)$ has a pole for any $\Gamma > 0$. The pole is simple and therefore

$$S_0(t) \simeq \alpha_2(\Gamma) e^{C_2(\Gamma)t} \quad (83)$$

when $t \gg 1$, with $C_2(\Gamma)$ and $\alpha_2(\Gamma)$ implicitly determined from

$$\Phi_2[C_2(\Gamma)] = \Gamma, \quad \frac{1}{\alpha_2(\Gamma)} = \left. \frac{d\Phi_2}{ds} \right|_{s=C_2(\Gamma)} \quad (84)$$

Combining (81) and (83) we obtain

$$N(t) \simeq A_2(\Gamma) e^{2C_2(\Gamma)t}, \quad A_2(\Gamma) = \frac{\Gamma \alpha_2(\Gamma)}{C_2(\Gamma)}^2 \quad (85)$$

Using the asymptotic

$$\Phi_2(s) = \frac{2\pi}{\ln(16/s)} + O\left(\frac{s^2}{\ln(1/s)}\right) \quad (86)$$

and (84) we find $C_2(\Gamma) \simeq 16e^{-2\pi/\Gamma}$ when $0 < \Gamma \ll 1$. Thus when $\Gamma \ll 1$, the growth remains exponential but has a very small amplitude in the exponent:

$$\lim_{t \rightarrow \infty} \frac{\ln N(t)}{t} = 32e^{-2\pi/\Gamma} \quad (87)$$

4.2. High dimensions

The functions $\Phi_d(s)$ are monotonically increasing functions of s in all dimensions and $\Gamma_d = \Phi_d(0) > 0$ in all dimensions apart from $d = 2$, see figure 4. We already know $\Gamma_1 = 2$ and $\Gamma_2 = 0$. The critical input rate in three dimensions can be expressed via the Euler's gamma function

$$\Gamma_3 = \frac{3}{\pi} \Gamma\left(\frac{5}{6}\right) \cdot \Gamma\left(\frac{2}{3}\right)^2 \quad (88)$$

The critical input rate in four dimensions can be expressed through a Meijer G-function (see [29, 30] for the definition of the Meijer G-functions):

$$\Gamma_4 = \frac{4\pi}{\text{MeijerG}\left[\left\{\{1, 1\}, \{1, 1\}\right\}, \left\{\frac{1}{2}, \frac{1}{2}\right\}, \left\{\frac{1}{2}, \frac{1}{2}\right\}\right], 1} \quad (89)$$

Here are a few numerical values of the critical input rate $\Gamma_d = \Phi_d(0)$:

$$\begin{aligned} \Gamma_1 &= 2 \\ \Gamma_2 &= 0 \\ \Gamma_3 &= 2.23104529048681\dots \\ \Gamma_4 &= 2.2155052677337\dots \\ \Gamma_5 &= 2.65391372999969\dots \\ \Gamma_6 &= 2.831160419094839\dots \\ \Gamma_7 &= 3.07421878003498\dots \end{aligned} \quad (90)$$

Note oscillations depending on the parity of d . For small d these oscillations are particularly notable and only for $d \geq 4$ the critical input rates Γ_d exhibit a monotonic growth when the spatial dimension increases. Using (75) and the small x expansion of the Bessel function

$$J_0(x) = 1 - \frac{x^2}{4} + \dots \quad (91)$$

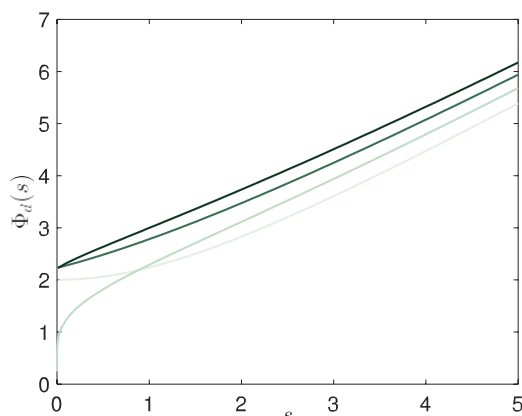


Figure 4. The functions $\Phi_d(s)$ for $d = 1, 2, 3, 4$. The curves are asymptotically parallel and go from light to dark (or bottom to top when $s \gg 1$) as d increases, see (93).

one can determine the large d behavior of the critical input rate:

$$\Gamma_d \simeq \frac{4d}{\pi} \quad (92)$$

Combining (75) and (91) one also finds the large s asymptotic of $\Phi_d(s)$:

$$\Phi_d(s) = s + \frac{2d}{s} + \dots \quad (93)$$

This large s behavior helps to identify the curves in figure 4. It also shows that the effective multiplication rate $C_d(\Gamma)$ appearing in (7), see also (97) below, behaves as

$$C_d(\Gamma) = \Gamma - \frac{2d}{\Gamma} + \dots \quad (94)$$

when $\Gamma \gg 1$.

Below we show that $N(t)$ is indeed described by (7) in the large time limit.

4.2.1. The supercritical regime: $\Gamma > \Gamma_d$. In this region in $d \geq 3$ dimensions, the Laplace transform $\hat{S}_0(s)$ has a simple pole at $s = C_d(\Gamma) > 0$ implying an exponential long time behavior

$$S_0(t) \simeq \alpha_d(\Gamma) e^{C_d(\Gamma)t} \quad (95)$$

with $C_d(\Gamma)$ and $\alpha_d(\Gamma)$ implicitly determined from

$$\Phi_d[C_d(\Gamma)] = \Gamma, \quad \frac{1}{\alpha_d(\Gamma)} = \frac{d\Phi_d}{ds} \Big|_{s=C_d(\Gamma)} \quad (96)$$

Thus the average total number of bosons exhibits an exponential growth

$$N(t) \simeq A_d(\Gamma) e^{2C_d(\Gamma)t}, \quad A_d(\Gamma) = \frac{\Gamma \alpha_d(\Gamma)}{C_d(\Gamma)}^2 \quad (97)$$

4.2.2. *The critical case:* $\Gamma = \Gamma_d$. At the critical point, the Laplace transform $\hat{S}_0(s)$ has a simple pole at the origin, namely $\hat{S}_0(s) \approx 1/(\beta_d s)$, from which

$$S_0(t) \approx \frac{1}{\beta_d}, \quad \beta_d = \frac{d\Phi_d}{ds} \Big|_{s=0} \tag{98}$$

leading to

$$N(t) \approx B_d^{\text{crit}} t^2, \quad B_d^{\text{crit}} = 2(\Gamma_d/\beta_d)^2 \tag{99}$$

In three dimension \int_0^∞

$$\beta_3 = (\Gamma_3)^2 \int_0^\infty duu [J_0(2u)]^3$$

Using identities

$$\int_0^\infty duu [J_0(2u)]^3 = \frac{1}{3} \int_0^\infty du [J_1(u)]^3 = \frac{1}{2\pi} \frac{\sqrt{3}}{3}$$

and (88) we express β_3 through the Euler's gamma function

$$\beta_3 = \frac{3\sqrt{3}}{2\pi^3} \Gamma\left(\frac{5}{6}\right) \cdot \Gamma\left(\frac{2}{3}\right)^4 = 0.45737905988493\dots \tag{100}$$

Using (88) and (100) we see that in three dimensions

$$B_3^{\text{crit}} = \frac{8}{27} \frac{\pi}{\Gamma\left(\frac{5}{6}\right) \cdot \Gamma\left(\frac{2}{3}\right)^4} = 5.28751612048\dots \tag{101}$$

Here are numerical values for β_d in the range $4 \leq d \leq 13$:

$$\begin{aligned} \beta_4 &= 1.89180068997\dots \\ \beta_5 &= 0.58095222806\dots \\ \beta_6 &= 0.67480419748\dots \\ \beta_7 &= 0.61631056140\dots \\ \beta_8 &= 0.63335480913\dots \\ \beta_9 &= 0.62600792587\dots \\ \beta_{10} &= 0.62977975271\dots \\ \beta_{11} &= 0.62908952670\dots \\ \beta_{12} &= 0.63021496135\dots \\ \beta_{13} &= 0.63047523664\dots \end{aligned} \tag{102}$$

Oscillations depending on the parity of d are even more pronounced than for the critical input rate Γ_d and only after $d \geq 11$ the quantities β_d become increasing functions of the dimensionality. Using (75) and (91) one establishes the saturation

$$\lim_{d \rightarrow \infty} \beta_d = \frac{2}{\pi}$$

of the quantities β_d in the large d limit.

4.2.3. The subcritical domain: $\Gamma < \Gamma_d$. Below the critical point, the Laplace transform $\hat{S}_0(s)$ has two simple poles at $s = \pm i\sigma_d(\Gamma)$

$$\int_0^\infty du \cos\{\alpha_d(\Gamma)u\} [J_0(2u)]^d = \frac{1}{\Gamma} \quad (103)$$

The contribution of these two poles into the inverse Laplace transform leads to the oscillating leading behavior similar to (43), namely

$$S_0(t) \simeq \Gamma^{-1} \sqrt{B_d(\Gamma)} \sin [t\sigma_d(\Gamma)] \quad (104)$$

Using (28) and (104) we arrive at $N(t) \simeq B_d(\Gamma)t^2$ as stated in (7).

5. Density profile in high dimensions

Using

$$\rho_0(t) = 2\Gamma \int_0^t dt' |S_0(t')|^2$$

and already established results for $S_0(t)$ we arrive at

$$\rho_0(t) \simeq \begin{cases} \Gamma^{-1} A_d(\Gamma) C_d(\Gamma) e^{2C_d(\Gamma)t} & \Gamma > \Gamma_d \\ \Gamma_d^{-1} B_d^{\text{crit}} t & \Gamma = \Gamma_d \\ \Gamma^{-1} B_d(\Gamma) t & \Gamma < \Gamma_d \end{cases} \quad (105)$$

describing the asymptotic growth of the density at the origin when $d \geq 3$. Comparing with (7) we see that in the supercritical regime the fraction of bosons at the origin approaches $\Gamma^{-1} C_d(\Gamma)$ as $t \rightarrow \infty$. Thus we have an intriguing spatial counterpart of Bose–Einstein condensation.

Let us analyze the entire density profile. We limit ourselves to the supercritical regime. We begin with the square lattice. In this situation $\Gamma_2 = 0$, so there is only supercritical regime. We must solve the following equation

$$\frac{dS_{m,n}}{dt} = i [S_{m+1,n} + S_{m-1,n} + S_{m,n+1} + S_{m,n-1}] + \Gamma \delta_{m,0} \delta_{n,0} S_{m,n} \quad (106)$$

We know that $S_{0,0}(t) \propto e^{C_2(\Gamma)t}$, see section 4.1. This together with the behavior of the density in the supercritical regime in one dimension suggest to seek the general solution of (106) in the form

$$S_{m,n}(t) = F_{m,n} e^{C_2(\Gamma)t} \quad (107)$$

Plugging this ansatz into (106) we obtain

$$F_{m+1,n} + F_{m-1,n} + F_{m,n+1} + F_{m,n-1} = -iC_2(\Gamma)F_{m,n} + i\Gamma\delta_{m,0}\delta_{n,0}F_{m,n} \quad (108)$$

Taking into account that $F_{1,0} = F_{-1,0} = F_{0,1} = F_{0,-1}$ due to symmetry we simplify (108) to

$$4F_{1,0} = i[\Gamma - C_2(\Gamma)]F_{0,0} \quad (109)$$

at the origin. Thus the density in the nearest-neighbor sites of the origin is

$$\frac{\rho_{1,0}}{\rho_{0,0}} = \frac{\Gamma - C_2(\Gamma)}{4} \quad (110)$$

Since $\Gamma - C_2(\Gamma) \simeq 4/\Gamma$ for $\Gamma \gg 1$, see (94), we obtain

$$\frac{\rho_{1,0}}{\rho_{0,0}} \simeq \Gamma^{-2} \quad \text{when } \Gamma \rightarrow \infty \quad (111)$$

Simulations indicate that $F_{m,n}$ is remarkably anisotropic, namely it quickly vanishes outside the diagonal $m = n$ and co-diagonal $m = -n$; along the diagonal and co-diagonal, $F_{m,n}$ is also quickly decaying when the separation from the origin increases; see figure 5. Let us try to understand these properties using approximate techniques. Consider for concreteness the positive quadrant $\{(m, n) \mid m > 0, n > 0\}$ and assume that $C_2 \ll 1$. This latter (technical) assumption insures that the decay along the diagonal is slow (albeit still exponential as we shall derive) and this allows to employ continuum methods. Thus we make the ansatz

$$F_{m,n} = i^{m+n}\Phi(m, n) \quad (112)$$

and treat $\Phi(m, n)$ as a function of continuous variables—this is justified when $m \gg 1$ and $n \gg 1$ if additionally $C_2 \ll 1$. Plugging the ansatz (112) into (108) we obtain

$$\Phi(m-1, n) - \Phi(m+1, n) + \Phi(m, n-1) - \Phi(m, n+1) = C_2\Phi(m, n)$$

which becomes

$$(\partial_m + \partial_n)\Phi + \frac{1}{2}C_2\Phi = 0 \quad (113)$$

in the continuum approximation. Introducing the variables

$$u = m - n, \quad v = m + n \quad (114)$$

we recast (113) into $\partial_v\Psi + \frac{1}{4}C_2\Psi = 0$ for $\Psi(u, v) = \Phi(m, n)$. Thus

$$\Psi(u, v) = \chi(u)e^{-C_2v/4} \quad (115)$$

with arbitrary $\chi(u)$. We haven't computed $\chi(u)$, but assuming it quickly vanishes as $|u|$ increases, this would explain numerical observations (shown in figure 5) that the density

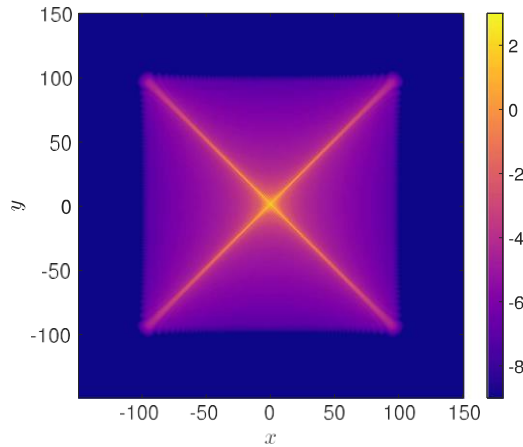


Figure 5. The density on a 300×300 square lattice at time $t = 50$ for $\Gamma = 1$. The color axis is logarithmic to resolve any structure away from the exponentially large density on the (co)-diagonal.

is mostly concentrated along the diagonal and co-diagonal. Moreover, (115) supports the exponential decay along the diagonal and co-diagonal which we observe numerically.

An exact analysis of (108) is possible. Applying the Fourier transform

$$F(p, q) = \sum_{m=-\infty}^{\infty} \sum_{n=-\infty}^{\infty} F_{m,n} e^{-ipm} e^{-iqn} \tag{116}$$

to (108) we find a neat expression

$$F(p, q) = \frac{\Gamma F_{0,0}}{C_2(\Gamma) - 2i(\cos p + \cos q)} \tag{117}$$

leading to the integral representation

$$F_{m,n} = \frac{1}{(2\pi)^2} \int_0^{2\pi} \int_0^{2\pi} dp dq \frac{\Gamma F_{0,0} e^{ipm} e^{iqn}}{C_2(\Gamma) - 2i(\cos p + \cos q)} \tag{118}$$

Euclidean versions of the integrals similar to those appearing in (117) and (118) are known as the lattice Green functions, see e.g. [28, 31–33] and references therein. These lattice Green functions can be expressed through special functions for a very few lattices, and even when this is possible the resulting formulas tend to be extremely complicated. For instance, for the square lattice the corresponding Green function has been expressed [33] through the hypergeometric function ${}_5F_4$, but extracting asymptotic behaviors from these exact formulas appears rather difficult.

Generally on the \mathbb{Z}^d lattice we have $S_n(t) = F_n e^{C_d(\Gamma)t}$ in the supercritical regime with

$$F_n = \int dq \frac{\Gamma F_{0,0} e^{iq \cdot n}}{C_d(\Gamma) - 2i \sum_{1 \leq a \leq d} \cos q_a} \tag{119}$$

J. Stat. Mech. (2020) 063101

where $\int dq$ is defined via (73b). The density ρ_0' in the nearest-neighbor sites of the origin is given again by a rather simple formula

$$\frac{\rho_0'}{\rho_0} = -C \frac{d}{\Gamma \lambda d} \Gamma^2 \quad (120)$$

6. Microscopic model

We have given exact analytic expressions, confirmed by numerical simulations, that show there is exponential growth of the number of particles above a certain critical injection rate Γ_c . But, how can we rationalize this? The Lindblad equation (1) describes the evolution of the ensemble average of a set of quantum trajectories, each evolving under a Hamiltonian H , while being subjected to a Poisson process that injects particles with an average rate Γ . If injection events occur at a fixed rate, it appears impossible to get an exponential growth. Let's try to resolve this apparent paradox by constructing a microscopic model that gives rise to Lindbladian dynamics (1). For Lindbladian (2), the dissipative part of the Lindblad equation (1) is quadratic. As a consequence, we expect that there exists a simple bilinear Hamiltonian for the system and reservoir that gives rise to the dissipative Markovian dynamics once the reservoir is traced out. Moreover, everything can be understood on the level of the Heisenberg equations of motion for the bosonic field operators. Before we investigate those equations for the closed system + reservoir dynamics, let's have a look at the equations of motion for the Lindblad dynamics. Recall that the Lindblad equation for observables in the Heisenberg picture is given by

$$\partial_t O = i[H, O] + 2L^\dagger O L - \{L^\dagger L, O\}. \quad (121)$$

Consequently for $O = b_i$, we find

$$\partial_t b_i = i[H, b_i] + \Gamma \delta_{i,0} b_i, \quad (122)$$

which is simply equation (13). The most naive model would correspond to

$$H_{\text{naive}} = H + \sum_i \omega_i a_i^\dagger a_i + \sum_i g_i (b_0^\dagger a_i + a_i^\dagger b_0), \quad (123)$$

where a_i are bosonic bath annihilation operators. By carefully choosing the spectrum ω_i and the coupling g_i , one can make sure the reduced dynamics becomes Markovian, i.e. one needs to guarantee that the noise spectral density is white such (q.v. expression (126)). The interaction term annihilates particles from the bath and puts them in the system. While it seems natural that this would lead to the Lindbladian (2), when we start with a bath that contains a lot of particles, we will now show it does not. The Heisenberg equations of motion for the bath degrees of freedom are

$$i\partial_t a_i = \omega_i a_i + g_i b_0. \quad (124)$$

This can readily be solved and we can simply substitute its solution into the Heisenberg equation of motion of the system operators, yielding

$$\partial_t b_i = i[H, b_i] - \delta_{i,0} \int_0^t ds \sum_j g_j^2 e^{-i\omega_j(t-s)} b_j(s) - i\delta_{i,0} \sum_j g_j e^{-i\omega_j t} a_j(0) \quad (125)$$

Taking the thermodynamic limit for the bath degrees of freedom, such that

$$\sum_j g_j^2 e^{-i\omega_j t} \rightarrow \Gamma \delta(t-s), \quad (126)$$

we arrive at

$$\partial_t b_i = i[H, b_i] - \Gamma \delta_{i,0} b_i + \delta_{i,0} f(t) \quad (127)$$

Here $f(t)$ is a stochastic driving term that depends on the initial state of the reservoir and the exact nature of the couplings $\sqrt{g_i}$. If we start with a reservoir that has N particles, the stochastic driving term $f \sim \sqrt{N}$. It will pump particles into the system, however, the self-interaction that the system picks up by interacting with the bath has the opposite sign of that in the Lindblad equation (122), i.e. it removes particles from the system rather than injecting them. Only the stochastic drive will inject particles. As a consequence, H_{naive} does not describe the Lindblad dynamics for the system. To generate the desired dynamics, we need to flip the sign of the self-interaction term. This can be done by swapping the bath creation and annihilation operators:

$$H_{\text{Matthew}} = H + \sum_i \omega_i a_i^\dagger a_i + \sum_i g_i (b_0^\dagger a_i^\dagger + a_i b_0) \quad (128)$$

Going through the same exercise as before, we derive the equation of motion

$$\partial_t b_i = i[H, b_i] + \Gamma \delta_{i,0} b_i + \delta_{i,0} f(t) \quad (129)$$

We can always initialize the bath in the vacuum state with no particles. The latter would make $f \neq 0$ leading to equation (122). Thus, we can think of the Lindbladian (2) in terms of H_{Matthew} which instead of removing a particle from the reservoir and putting it into the system creates a pair of particles, one in the reservoir and one in the system. The term $\Gamma b_i \delta_{i,0}$ in equation (129) triggered by the input now comes with positive sign leading to the rich get richer, or quantum Matthew effect. The total particle number is not conserved, which makes it possible to sustain this exponential growth. Moreover, the transition from quadratic to exponential growth can be interpreted as a transition from a dynamically stable to a dynamically unstable system (128). By itself, this Hamiltonian is unphysical in the dynamically unstable regime as it is also thermodynamically unstable, i.e. the ground state has unbounded energy. However, the Hamiltonian can always be thought of as an effective Hamiltonian arising as the Bogoliubov description of a more complex problem. Examples of the latter, in which similar physics appears,

include the dynamical Casimir effect [34] and parametric instabilities in driven systems [35]. We also notice that an open *classical* system of non-interacting random walks multiplying on a ‘fertility’ site is somewhat similar to the open quantum system described by the Hamiltonian (128) and it exhibits similar behaviors (see [36] and references therein).

7. Conclusions

Open quantum systems driven by a localized source demonstrate the dramatic difference between fermions and bosons. In the case of identical fermions, the behavior is rather predictable [15, 17], e.g., the total number of fermions grows linearly in time and only the dependence of the fermion growth rate on the input rate is unusual, viz it decays as $1/\Gamma$ when the source becomes strong which is a manifestation of the quantum Zeno effect. For bosons, the growth is super-linear: quadratic in time when $\Gamma < \Gamma_d$ and exponential when $\Gamma > \Gamma_d$. The tendency of identical bosons to bunch is well-known in the context of closed quantum systems, with Bose–Einstein condensation being the beautiful illustration of this phenomenon. Another way to express the exponential growth in our open quantum system of identical bosons is to think about it in terms of the microscopic ‘Matthew’ Hamiltonian (see (128)) leading to rich get richer, or the quantum Matthew effect. Our work indicates that in the context of open quantum systems the difference between fermions and bosons can be more spectacular than for closed quantum systems.

We analyzed the asymptotic behavior of the average total number of injected bosons. Needless to say, one would like to probe the behavior of higher cumulants, and to study the entire distribution function $P(N, t)$ or the full counting statistics. A self-averaging behavior is anticipated in the case of identical fermions, so the average total number of injected fermions provides an asymptotically complete description. In the case of non-interacting bosons, self-averaging or the lack of it is an interesting issue. At the transition point $\Gamma = \Gamma_d$, the fluctuations could be especially pronounced.

Another obvious extension is related to the spatial distribution of bosons. We determined the density profile in one dimension. In higher dimensions, particularly in the supercritical regime, we derived exact integral representations. Extracting asymptotic behaviors from these integral representation is an intriguing challenge since the numerically observed spatial distribution is strikingly anisotropic (see figure 5). We also emphasize that in the supercritical regime the fraction of bosons at the origin approaches to a constant, namely to $\Gamma^{-1}C_d(\Gamma)$. This could be interpreted as Bose–Einstein condensation in a spatially localized state.

An open quantum system of bosons driven by a localized source has been previously studied in reference [16] where a possibility of an exponential growth has been discovered. Our analysis is much more detailed as the lattice system appears to be more amenable to analytical work. Intriguingly, the linear in time growth occurs only when $t \ll 1$, while for $t \gg 1$ even in the sub-critical regime the growth is quadratic. It would be interesting to find an intuitive understanding of the quadratic $N \propto t^2$ growth law.

An intriguing feature of our open system of bosons is a phase transition occurring for all $d \geq 2$. The two-dimensional case is special in numerous problems where the mathematical framework relies on the Laplacian, e.g. in *classical* diffusive systems driven by a localized source the two-dimensional behaviors could be subtle, see e.g. [37, 38]. Still, the peculiar role of $d = 2$ in the present situation is striking. We established this special behavior for the square lattice, so it would be interesting to probe its validity for other two-dimensional lattices.

Acknowledgments

PLK thanks the Institut de Physique Théorique and the Los Alamos National Laboratory for hospitality. KM is grateful to Michel Bauer, Jean-Marc Luck and Tomaž Prosen for illuminating discussions. DS acknowledges support from the FWO as post-doctoral fellow of the Research Foundation–Flanders.

References

- [1] Gorini V, Kossakowski A and Sudarshan E C G 1976 Completely positive dynamical semigroups of N-level systems *J. Math. Phys.* **17** 821
- [2] Lindblad G 1976 On the generators of quantum dynamical semigroups *Commun. Math. Phys.* **48** 119
- [3] Breuer H-P and Petruccione F 2002 *The Theory of Open Quantum Systems* (Oxford: Oxford University Press)
- [4] Manzano D 2019 A short introduction to the Lindblad master equation (arXiv:1906.04478)
- [5] Scully M O and Zubairy M S 1997 *Quantum Optics* (Cambridge: Cambridge University Press)
- [6] Haroche S and Raimond J-M 2006 *Exploring the Quantum: Atoms, Cavities, and Photons* (Oxford: Oxford University Press)
- [7] Nielsen M A and Chuang I L 2000 *Quantum Computation and Quantum Information* (Cambridge: Cambridge University Press)
- [8] Preskill J 2015 Lecture notes for physics 219: quantum computation Ch 3 (unpublished) <http://www.theory.caltech.edu/people/preskill/ph229/>
- [9] Bauer M, Bernard D and Jin T 2017 Stochastic dissipative quantum spin chains (I): quantum fluctuating discrete hydrodynamics *SciPost Phys.* **3** 033
- [10] Bernard D, Jin T and Shpielberg O 2018 Transport in quantum chains under strong monitoring *Europhys. Lett.* **121** 60006
- [11] Breuer H-P, Laine E-M, Piilo J and Vacchini B 2016 Non-Markovian dynamics in open quantum systems *Rev. Mod. Phys.* **88** 021002
- [12] Spohn H 1977 An algebraic condition for the approach to equilibrium of an open N-level system *Lett. Math. Phys.* **2** 33
- [13] Kosloff R 2013 Quantum thermodynamics: a dynamical viewpoint *Entropy* **15** 2100
- [14] Brandner K and Seifert U 2016 Periodic thermodynamics of open quantum systems *Phys. Rev. E* **93** 062134
- [15] Krapivsky P L, Mallick K and Sels D 2019 Free fermions with a localized source *J. Stat. Mech.* 2019 113108
- [16] Butz M and Spohn H 2010 Dynamical phase transition for a quantum particle source *Ann. Henri Poincaré* **10** 1223
- [17] Fröml H, Chiocchetta A, Kollath C and Diehl S 2019 Fluctuation-induced quantum Zeno effect *Phys. Rev. Lett.* **122** 040402
- [18] Fröml H, Muckel C, Kollath C, Chiocchetta A and Diehl S 2020 Ultracold quantum wires with localized losses: many-body quantum Zeno effect *Phys. Rev. B* **101** 144301
- [19] Barmettler P and Kollath C 2011 Controllable manipulation and detection of local densities and bipartite entanglement in a quantum gas by a dissipative defect *Phys. Rev. A* **84** 041606
- [20] Zezyulin D A, Konotop V V, Barontini G and Ott H 2012 Macroscopic Zeno effect and stationary flows in nonlinear waveguides with localized dissipation *Phys. Rev. Lett.* **109** 020405
- [21] Kordas G, Wimberger S and Witthaut D 2013 Decay and fragmentation in an open Bose–Hubbard chain *Phys. Rev. A* **87** 043618

- [22] Kiefer-Emmanouilidis M and Sirker J 2017 Current reversals and metastable states in the infinite Bose–Hubbard chain with local particle loss *Phys. Rev. A* **96** 063625
- [23] Sels D and Demler E 2020 Thermal radiation and dissipative phase transition in a BEC with local loss *Ann. Phys.* **412** 168021
- [24] Labouvie R, Santra B, Heun S and Ott H 2016 Bistability in a driven-dissipative superfluid *Phys. Rev. Lett.* **116** 235302
- [25] Müllers A, Santra B, Baals C, Jiang J, Benary J, Labouvie R, Zezyulin D A, Konotop V V and Ott H 2018 Coherent perfect absorption of nonlinear matter waves *Sci. Adv.* **4** eaat6539
- [26] Krapivsky P L, Luck J M and Mallick K 2014 Survival of classical and quantum particles in presence of traps *J. Stat. Phys.* **154** 1430
- [27] Erdélyi A, Magnus W, Oberhettinger F and Tricomi F G 1953 *Tables of Integral Transforms* vol 1 (New York: McGraw-Hill Book Company)
- [28] Hughes B D 1995 *Random Walks and Random Environments. Volume 1: Random Walks* (Oxford: Clarendon)
- [29] Bateman H and Erdélyi A 1953 *Higher Transcendental Functions* vol 1 (New York: McGraw-Hill Book Company)
- [30] Askey R A and Olde Daalhuis A B 2010 *NIST Handbook of Mathematical Functions* ed F W J Olver, D M Lozier, R F Boisvert and C W Clark (Cambridge: Cambridge University Press)
- [31] Joyce G S 2003 Singular behavior of the lattice Green function for the d-dimensional hypercubic lattice *J. Phys. A* **36** 911
- [32] Guttmann A J 2010 Lattice Green’s functions in all dimensions *J. Phys. A* **43** 305205
- [33] Ray K 2014 Green’s function on lattices (arXiv:1409.7806)
- [34] Michael M H, Schmiedmayer J and Demler E 2019 From the moving piston to the dynamical Casimir effect: Explorations with shaken condensates *Phys. Rev. A* **99** 053615
- [35] Lellouch S, Bukov M, Demler E and Goldman N 2017 Parametric Instability Rates in Periodically Driven Band Systems *Phys. Rev. X* **7** 021015
- [36] Bauer M, Krapivsky P L and Mallick K 2019 Random walk through a fertile site (arXiv:1907.12822)
- [37] Krapivsky P L 2012 Symmetric exclusion process with a localized source *Phys. Rev. E* **86** 041103
- [38] Krapivsky P L and Stefanovic D 2014 Lattice gases with a point source *J. Stat. Mech.* 2014 P09003